Improving Vehicular Traffic Simulations Using Real-Time Information on Environmental Conditions

Lars Habel
and Michael Schreckenberg
Physics of Transport and Traffic
Universität Duisburg-Essen
47048 Duisburg, Germany
Email: {lars.habel,michael.schreckenberg}@uni-due.de

Christoph Ide
and Christian Wietfeld
Communication Networks Institute
Technische Universität Dortmund
44227 Dortmund, Germany
Email: {christoph.ide,christian.wietfeld}@tu-dortmund.de

***Abstract*—This contribution illustrates the benefit of incorporating real-time environmental data into highway traffic information systems and describes the modelling and integration of weather conditions into a complex microscopic traffic simulation. Using stationary measured weather data as an example, the achieved results show the potential extended Floating Car Data (xFCD) - submitted to the traffic information system by cellular communication - can have for traffic simulation. Therefore, an estimation about the expected communication network load is given, when xFCD equipped vehicles have become prevalent.**

I. Introduction

In the last two decades, availability and capacity of mobile communication systems have grown rapidly. With this technology, the development of applications which use data from many distributed devices has become possible. As a part of so-called Vehicular-2-X Communication [1], much research has been done to make use of *Floating Car Data* (FCD) in the fields of traffic information and improvement. Usually, FCD consists of position and velocity of the transmitting vehicle at a certain point of time. With these observables, it is possible to perform traffic state detection [2], which is especially useful on road sections, where stationary traffic detectors are missing, damaged or not accessible. In this context, FCD is already used in commercial traffic information systems, also in the form of *Floating Phone Data* (FPD) [3].

Apart from gaining and distributing traffic state information, FCD has become attractive for researchers to develop concepts for traffic improvement. Here, FCD is understood to comprise not only position and velocity but every needed information that is measurable or evaluable by the vehicle. This data is usually called *extended Floating Car Data* (xFCD) [4]. Concepts using xFCD often aim to improve traffic safety, for example with the transmission of hazardous road conditions [5] or temporary traffic signs [6] to a server or vehicles nearby. Other concepts aim to improve the cooperation between neighboring vehicles. Therefore, we proposed the use of vehicular ad-hoc networks (VANETs) [7], while server-based concepts often rely on cellular communication networks (e.g. UMTS/LTE [8]). As empirical xFCD is still almost unavailable on a large scale, most of the work in this field is based on simulations.

Machine-Type Communication [9] like the transmission of xFCD is a recent topic in the development of modern cellular communication systems [8]. The drawback of providing the xFCD by cellular communication, is the interaction between MTC and "traditional" Human-to-Human (H2H) traffic in the network. In [10], we therefore presented a channel-aware transmission approach to minimize the negative impact of xFCD transmissions on other LTE users. In [11], we provided a further optimization using a prioritization strategy for xFCD transmissions.

Modern vehicles often are equipped with sensor-based assistant systems like automatic driving light control or rain-sensing windscreen wipers. In this contribution, we propose a new concept for transmitting such xFCD as well as stationary measured environmental data to a server, which feeds the data into a cellular-automaton (CA) based microscopic vehicular traffic simulation [12] at runtime. As a use case of stochastic transport processes, CA-based traffic models have been interesting for physicists since about twenty years. The development of the three-phase traffic theory by Kerner [13] has since led to realistic traffic models, which can reproduce many empirical findings. Therefore they are well-suited for the use in traffic information systems.

In Section II, we present new empirical findings about the influence of surface wetness on vehicular traffic to parametrize the traffic model. In Section III, we describe how environmental information from stationary detectors and xFCD can be integrated into vehicular traffic simulations and present simulation results. Also, we provide a quantification of the additional communication network payload resulting from the xFCD transmissions.

978-1-5090-1701-0/16/$31.00 ©2016 IEEE

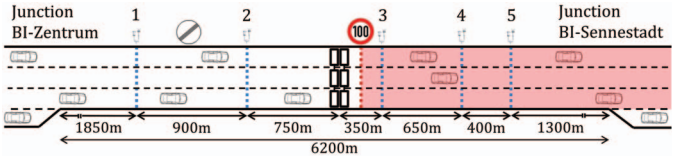

Fig. 1. Sketch of the analyzed section of the German highway A2.

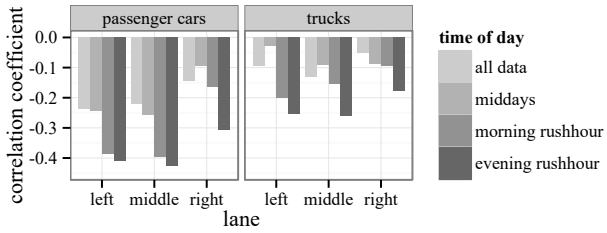

Fig. 2. Correlation coefficients for the relationship between vehicle type-specific velocities and water film thickness.

II. Data Sources and Empirical Measurements

We investigated 1-minute weather data from 303 days between 1 July 2012 and 1 May 2013 as well as the corresponding traffic data from a $6200\,\mathrm{m}$ long section of the German highway A2 (cf. Fig. 1). Due to a hilly road profile and the risk of ice build-up during winter, the section is equipped with five weather stations. One traffic loop per lane provides the vehicular traffic data.

A. Influence of water film thickness on traffic

Measuring precipitation by weather sensors is usually performed either using a simple rain water collector, which measures the amount of rain in a period of time, or by sensors within the road surface and optical systems, which measure the water film thickness at a point on the road at a certain time. Data measured on the road surface incorporates properties of the road surface at the point of measurement: Surface damage can increase the thickness of the water film, while the presence of open graded asphalt can reduce it considerably. There might also be a water film on the road when rainfall already has ended or when fallen snow is thawing. Hence, the intensity of spray produced by preceding vehicles depends not only on the rain intensity, but also on the surface quality. This property makes the water film sensor more valuable than a simple rain intensity sensor. Additionally, it is easier to compare its measurements with data from rain-sensing windscreen wipers provided by vehicles with xFCD technology, because they react on spray as well.

To motivate this contribution, the impact of surface wetness on velocities is quantified in Fig. 2 by means of Pearson's product-matrix correlation coefficients for different

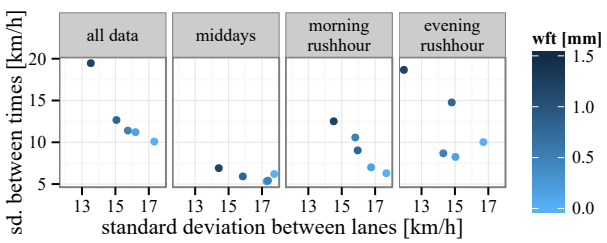

Fig. 3. Comparison of standard deviations of the passenger car velocity: Each point represents measurements at a certain water film thickness.

times of day[1]. With about -0.4 for passenger cars, the correlations are almost twice as high during morning and evening rush hours as they are at midday. This underlines the benefit of incorporating environmental information in traffic information systems for commuters.

B. Rain and the predictability of traffic

From theoretical approaches in the framework of the three-phase traffic theory [14], it is known that bad weather conditions can cause traffic breakdowns as other bottlenecks like on-ramps. In the present work, we address this topic by two data examinations.

Fig. 3 visualizes the relationship between the homogeneity of velocities and their predictability at a given water film thickness. The homogeneity of velocities can be described by calculating the standard deviation of the passenger car velocities from all lanes at a certain point of time and water film thickness. The averages of these values are used as x-value of the points in Fig. 3. High values represent high velocity differences between the lanes, which typically can be found at dry surface conditions. When the road surface is wet, the velocities synchronize like in the synchronized flow phase of the three-phase traffic theory. The predictability of a velocity can be expressed using the standard deviation of velocities measured at different times, but the same water film thickness. Based on the average passenger car velocity of the whole roadway, the y-values of the points in Fig. 3 represent this predictability for the given water film thickness. High values indicate that the set of average velocities contains a wide span of velocities, meaning that the velocity at a certain point of time is less predictable. This is often the case when the surface is wet, especially during the rush hours.

According to the three-phase traffic theory, there is an infinite number of road capacities (i.e. traffic flows measured downstream of a bottleneck) between a minimum capacity where the breakdown probability is 0 and a maximum capacity where it is 1 [13]. In Table I, we show how much the maximum capacity is influenced by surface

[1]Data subsets: Morning rush hour: 6:00 a.m. – 9:00 a.m., evening rush hour: 4:00 p.m – 7:00 p.m., midday: 11:00 a.m – 3:00 p.m. on regular working days without school holidays.

TABLE I
MAXIMUM VEHICULAR TRAFFIC FLOWS DEPENDING ON SURFACE WETNESS.

surface	range of water film thickness w	maximum flow
dry	$w \leq 0.15\,\mathrm{mm}$	$1960\,\mathrm{vehs/(h, lane)}$
damp	$0.15\,\mathrm{mm} < w < 0.9\,\mathrm{mm}$	$1720\,\mathrm{vehs/(h, lane)}$
wet	$w \geq 0.9\,\mathrm{mm}$	$1320\,\mathrm{vehs/(h, lane)}$

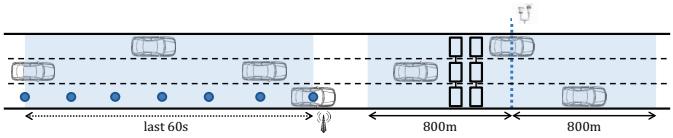

Fig. 4. Visualization of different strategies for incorporating environmental data into the simulation. Left: xFCD, right: stationary sensor.

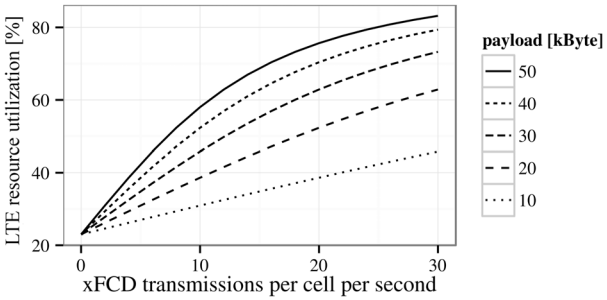

Fig. 5. Normalized LTE utilization as a function of the number of xFCD transmissions for different payload sizes. The results are gained using the parameters: $S = 50$, $c_M = 6$, $\lambda_H = 1/25\,\mathrm{s}$, $\mu_H = 1/120\,\mathrm{s}$ and $100\,\mathrm{kbit/s}$ H2H data rate.

wetness by means of maximum measured vehicular traffic flows, which have been obtained from free flow traffic within the 11-month data set. These values effectively are lower bounds of the maximum capacities of each type of surface wetness. Because of the limited amount of data and possible detection errors, measuring a maximum capacity itself is not possible. We therefore defined a threshold, meaning that Table I only shows flows that were reached more than ten times within 11 months.

III. PROVIDING ENVIRONMENTAL INFORMATION IN VEHICULAR TRAFFIC SIMULATIONS

Environmental conditions influence traffic mainly on a local scale, so they should be incorporated into the CA model using locally active model additions (cf. Fig. 4). This can e.g. be done by applying a locally different parameter set to the model.

A. Connection with real-time data

For stationary environmental detectors, a fixed area around the detector is sufficient. In the given data set, correlations between neighboring water film detectors stay very high (approx. 0.9) for detector distances between $650\,\mathrm{m}$ and about $1000\,\mathrm{m}$. Hence, we choose an extend of $800\,\mathrm{m}$ on both sides of the detector. Environmental data is transmitted every $60\,\mathrm{s}$.

In case of xFCD, a moving area behind a transmitting vehicle should be preferred. A transmitting vehicle driving with $v \approx 108\,\mathrm{km/s}$ covers an area of about $1800\,\mathrm{m}$ within $60\,\mathrm{s}$. This coverage is in very good agreement in space and time with that of stationary detectors. Start and end positions of all moving areas have to be recalculated before every update step. This can be performed with the algorithm

1) order all xFCD by vehicle position at transmission time (descending order)
2) remove all entries with timestamps older than $60\,\mathrm{s}$
3) start at the top of the list and begin an area
4) begin a new area, when the observed value changes, the distance between two entries exceeds $1000\,\mathrm{m}$ or a stationary covered area is reached.

The empirical findings presented in Section II are based on stationary sensors. In order to profit from the additional information in a traffic information system, the environmental conditions have to be determined in real-time at many different positions of the road network.

Therefore, we provide a quantification of the influence of xFCD transmissions with a different payload size on the utilization of the LTE network. For this purpose, a Markovian model we presented in [15] is used, that bases on a an extension of the Erlang B model [16]. By means of this multi-class Erlang loss model, the LTE uplink resource utilization is modeled in an analytic way. Thereby, different user classes representing H2H traffic and xFCD transmissions are considered. The j^{th} state of the model denotes the allocation of j resource blocks from the LTE uplink signal. Moreover λ_i and μ_i denote the mean arrival rate (e.g. number of xFCD transmissions per second for MTC) and mean service rate (e.g. xFCD transmission duration for MTC) of the i^{th} class.

According to Kaufman [17], the stationary distribution π_c, which characterizes the probability that c resource blocks are used, can be determined with

$$\pi_c = \frac{\widetilde{\pi}_c}{\sum_{k=0}^{C} \widetilde{\pi}_k} \quad \text{with} \quad \widetilde{\pi}_c = \begin{cases} 1 & c = 0 \\ \sum_{i=1}^{S} \frac{a_i c_i}{c} \widetilde{\pi}_{c-c_i} & c > 0\,, \end{cases} \tag{1}$$

where C is the overall number of resource blocks ($C = 100$ for a $20\,\mathrm{MHz}$ LTE cell), a_i the offered traffic of class i, c_i is the corresponding resources of class i and S is the number of service classes. Then, the traffic load Y which describes the average resource utilization can be calculated as

$$Y = \sum_{c=1}^{C} c\pi_c\,. \tag{2}$$

Details about the model can be found in [15].

In Fig. 5, the results of this model are presented regarding the normalized LTE utilization as a function of the number of xFCD transmissions per cell and second for

different payload sizes. It can be seen from the figure, that the load of the cellular network is significantly dependent on the size and the frequency of data transmissions. Thereby, also H2H traffic is served from the LTE network. This traffic is responsible for the $22\,\%$ basic load.

For a typical LTE deployment (cell radius $2.5\,\mathrm{km}$), a sufficient penetration rate of $5\,\%$ (cf. [2]), each vehicle transmits the xFCD every $10\,\mathrm{s}$, two motorways with three lanes per direction in the coverage of the LTE cell and a high traffic situation (50 vehicles per km and lane), on average 15 vehicles send xFCD per cell and second. For this scenario, the LTE cell is more than 50% utilized (cf. Fig. 5 for 30 kByte payload). This means that the information for this high traffic situation can be served by the network, but the traffic load generated by the vehicles is higher that the assumed load from H2H traffic.

B. Modelling environment-influenced driving

Vehicular motion is simulated using the microscopic traffic model presented by Lee *et al* [12] with our enhancements for multi-lane traffic [18] and slightly different parameters. The model by Lee *et al* contains a probabilistic element known from previously introduced CA-based traffic models, but in contrast to most of them, each vehicle n has limited accelerating and braking capabilities $a_n = 1$ and $D = 2$. The model uses a space discretization of $1\,\mathrm{cell} = 1.5\,\mathrm{m}$, each time step corresponds to $1\,\mathrm{s}$. Passenger cars occupy $l_\mathrm{P} = 5$ cells, their maximum velocity is $v_{\max,\mathrm{P}} = 23\,\mathrm{cells/s}$. Trucks are $l_\mathrm{L} = 10$ cells long and have a maximum velocity of $v_{\max,\mathrm{L}} = 16\,\mathrm{cells/s}$.

Empirical analyses of single-vehicle data have shown that time headways between succeeding vehicles rise in rainy conditions [19], because the mean velocities fall. The distance gap between vehicles remains unaffected [19], though. From this perspective, rising the minimum time look-ahead t_safe depending on the environmental conditions seems to be obvious [14]. Unfortunately, the given CA model would not reproduce this behavior, because the minimum gap would also rise, which only depends on t_safe. The minimum gap even does not depend on v_max. A simple adjustment of v_max according to the current environmental conditions would not be sufficient either, because the uncertainty shown in Section II (cf. Fig. 3) would not be reproduced.

Bringing uncertainty into a CA traffic model is usually done by randomized braking and non-accelerating. In the given CA model, the probability is controlled mainly by p_d, which is a constant real number. To reflect the varying intensity of environmental influences on traffic according to Section II, we introduce an additional environment-related randomization function $p_\mathrm{w}(w)$, which depends e.g. on the surface wetness w.

A microscopic traffic simulation that uses empirical real-time data performs three different tasks during an $1\,\mathrm{s}$ cycle: Update, measurement and tuning [20]. Regular vehicular movement is performed in the update stage.

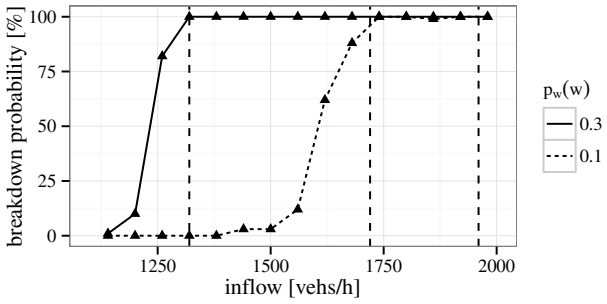

Fig. 6. Simulated breakdown probabilities for different $p_\mathrm{w}(w)$, measured at position $6850\,\mathrm{m}$ (averages from 100 simulation runs).

In the measurement stage, new simulation results are obtained and published each minute in a database. In the tuning stage, the simulation makes decisions and vehicular movements based on empirical real-time data e.g. from off- and on-ramps. These three stages should be separated from each other for programming reasons. Thus, we define an additional randomization *step*, that is performed independently in the tuning stage with

$$\hat{v}_n^{(t+1)} = \max\left\{0, v_n^{(t)} - D, v_n^{(t+1)} - D(w)\right\}, \qquad (3)$$

where $D(w) = 1$ if `(random-real)` $< p_\mathrm{w}(w)$, else $D(w) = 0$. The step is performed after $v_n^{(t+1)}$ has been obtained. $v_n^{(t)} - D$ ensures, that a vehicle does not brake harder than D in update and tuning stage together.

C. Simulation results

In the following, we provide a parametrization of $p_\mathrm{w}(w)$ for damp and wet road surfaces. Therefore, we performed simulations of traffic on a $10\,\mathrm{km}$ long three-lane highway section using the aforementioned rules. In each simulation, a constant inflow of vehicles at the upstream boundary between $600\,\mathrm{vehs/(h,lane)}$ and $2400\,\mathrm{vehs/(h,lane)}$ is used. Vehicles reaching the downstream boundary are simply taken off the road. $15\,\%$ of all vehicles are trucks, which are inserted in toto on the right lane. Between $6750\,\mathrm{m}$ and $8250\,\mathrm{m}$, the simulated road is affected by surface wetness according to Eq. (3). In each of the simulations, one of eight different values of $p_\mathrm{w}(w)$ between $p_\mathrm{w}(w) = 0.1$ and $p_\mathrm{w}(w) = 0.45$ is chosen. Surface wetness is switched on after $60\,\mathrm{min}$ of relaxation time.

A parametrization of $p_\mathrm{w}(w)$ can be obtained by measuring breakdown probabilities for different values of $p_\mathrm{w}(w)$. Traffic breakdowns were counted using the following criterion: A breakdown has occurred, when the passenger car velocity was lower than $65\,\mathrm{km/h}$ during $5\,\mathrm{min}$ within the first $30\,\mathrm{min}$ after the surface wetness had been switched on. Compared to the empirical data, this means that the velocity had to be $10\,\mathrm{km/h}$ lower than the mean empirical velocity on the right lane on a dry surface.

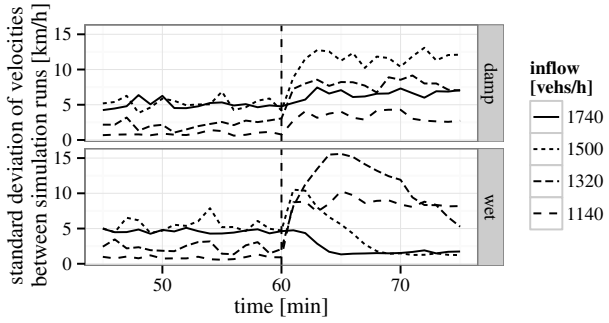

Fig. 7. Standard deviation of simulated velocity time series, measured at position $6850\,\mathrm{m}$ (averages from 100 simulation runs).

A subset of the resulting breakdown probability curves is displayed in Fig. 6. To find appropriate values of $p_\mathrm{w}(w)$ for damp and wet surfaces, we use the empirically measured maximum flows shown in Table I as an upper boundary to propose the parametrization

$$p_\mathrm{w}(w) = \begin{cases} 0.3 & \text{if } w \geq 0.9\,\mathrm{mm}, \\ 0.1 & \text{if } 0.15\,\mathrm{mm} < w < 0.9\,\mathrm{mm}, \\ 0 & \text{else.} \end{cases} \quad (4)$$

In Fig. 7, the influence of the proposed method on simulated traffic is visualized by means of the velocity standard deviations. At damp conditions, the standard deviations rise, which is in good agreement with the empirical data shown on the vertical axis of Fig. 3. At wet conditions, the deviations rise for inflows below the breakdown flow, but converge on a very low level for inflows of $1500\,\mathrm{vehs}/(\mathrm{h},\mathrm{lane})$ and higher. This behavior can be explained by a look at the model mechanics: First, the happening velocity reduction is not performed instantly after entering the area, because the model does not allow unlimited braking. Also, the model privileges vehicles driving in a row with the same speed under certain circumstances. These formations are disturbed by the additional randomized braking with Eq. (3). The all-disturbed state of the model exhibits a very narrow time headway distribution, leading to very homogeneous velocities and to jam emergence upstream of the area.

IV. Conclusion

In this contribution, we presented an approach to improve the reliability and accuracy of vehicular traffic information systems by using additional real-time environmental data from stationary and moving sensors.

The proposed strategy is able to reproduce the presented empirical findings based on the three-phase traffic theory. Therefore, it can be a valuable addition to microscopic simulations, which by now solely base on conventional vehicular traffic data. Also, the strategy is applicable in real-world LTE networks, because the additional xFCD utilization can fully be handled by the communication system.

Acknowledgment

LH and CI have been supported by Deutsche Forschungsgemeinschaft (DFG) within the Collaborative Research Center SFB 876 “Providing Information by Resource-Constrained Analysis”, project B4 “Analysis and Communication for the Dynamic Traffic Prognosis”.

We thank Straßen.NRW for providing the empirical data.

References

[1] R. Popescu-Zeletin, I. Radusch, and M. A. Rigani, *Vehicular-2-X Communication*. Springer, 2010.

[2] B. S. Kerner, C. Demir, R. G. Herrtwich, S. L. Klenov, H. Rehborn, M. Aleksic, and A. Haug, “Traffic State Detection with Floating Car Data in Road Networks,” in *8th International IEEE Conference on Intelligent Transportation Systems*, 2005, pp. 44–49.

[3] B. S. Kerner, H. Rehborn, R.-P. Schäfer, S. L. Klenov, J. Palmer, S. Lorkowski, and N. Witte, “Traffic Dynamics in Empirical Probe Vehicle Data studied with Three-Phase Theory: Spatiotemporal Reconstruction of Traffic Phases and Generation of Jam Warning Messages,” *Physica A*, vol. 392, no. 1, pp. 221–251, 2013.

[4] W. Huber, M. Lädke, and R. Ogger, “Extended floating-car data for the acquisition of traffic information,” in *6th World congress on intelligent transport systems*, 1999, pp. 1–9.

[5] M. Hauschild, “Weather and Road Surface Information and Hazard Warnings: Data content acquisition through advanced probe vehicle systems,” in *12th World congress on intelligent transport systems*, 2005.

[6] S. Messelodi, C. M. Modena, M. Zanin, F. G. De Natale, F. Granelli, E. Betterle, and A. Guarise, “Intelligent extended floating car data collection,” *Expert. Syst. Appl.*, vol. 36, no. 3, pp. 4213–4227, 2009.

[7] F. Knorr, D. Baselt, M. Schreckenberg, and M. Mauve, “Reducing Traffic Jams via VANETs.” *IEEE T. Vehicular Technology*, vol. 61, no. 8, pp. 3490–3498, 2012.

[8] G. Araniti, C. Campolo, M. Condoluci, A. Iera, and A. Molinaro, “LTE for vehicular networking: a survey,” *IEEE Commun. Mag.*, vol. 51, no. 5, pp. 148–157, 2013.

[9] “3GPP TR 36.888 - Study on Provision of Low-Cost MTC UEs Based on LTE,” 3rd Generation Partnership Project, jun. 2013. [Online]. Available: http://www.3gpp.org

[10] C. Ide, B. Dusza, M. Putzke, and C. Wietfeld, “Channel sensitive transmission scheme for V2I-based Floating Car Data collection via LTE,” in *2012 IEEE International Conference on Communications (ICC)*, 2012, pp. 7151–7156.

[11] C. Ide, L. Habel, T. Knaup, M. Schreckenberg, and C. Wietfeld, “Interaction between Machine-Type Communication and H2H LTE Traffic in Vehicular Environments,” in *2014 IEEE Vehicular Technology Conference (VTC Spring)*, 2014, pp. 1–5.

[12] H. K. Lee, R. Barlovic, M. Schreckenberg, and D. Kim, “Mechanical restriction versus human overreaction triggering congested traffic states,” *Phys. Rev. Lett.*, vol. 92, no. 23, p. 238702, 2004.

[13] B. S. Kerner, *Introduction to Modern Traffic Flow Theory and Control: The Long Road to Three-Phase Traffic Theory*. Springer, 2009.

[14] ——, “A theory of traffic congestion at heavy bottlenecks,” *J. Phys. A: Math. Theor.*, vol. 41, no. 21, p. 215101, 2008.

[15] C. Ide, B. Dusza, M. Putzke, C. Muller, and C. Wietfeld, “Influence of M2M communication on the physical resource utilization of LTE,” in *Wireless Telecommunications Symposium (WTS) 2012*, 2012, pp. 1–6.

[16] T. S. Rappaport, *Wireless Communications: Principles and Practice*, 2nd ed. Prentice Hall, 2002.

[17] J. Kaufman, “Blocking in a Shared Resource Environment,” *IEEE Trans. Commun.*, vol. 29, no. 10, pp. 1474–1481, 1981.

[18] L. Habel and M. Schreckenberg, “Asymmetric Lane Change Rules for a Microscopic Highway Traffic Model,” in *Cellular Automata*, ser. LNCS, J. Was, G. C. Sirakoulis, and S. Bandini, Eds., vol. 8751. Springer, 2014, pp. 620–629.

[19] A. Rahman and N. E. Lownes, “Analysis of rainfall impacts on platooned vehicle spacing and speed,” *Transport. Res. F*, vol. 15, no. 4, pp. 395–403, jul 2012.

[20] J. Brügmann, M. Schreckenberg, and W. Luther, “A verifiable simulation model for real-world microscopic traffic simulations,” *Simul. Model. Pract. Theory*, vol. 48, pp. 58–92, 2014.